interaction ($P = 0.165$, $P = 0.123$, $P = 0.637$, $P = 0.683$), respectively.

Self-rating

Two-way repeated-measures analysis of variance of the ratings showed a significant main effect of condition ($P < 0.001$) but not a significant main effect of drug ($P = 0.66$) or interaction ($P = 0.59$). In other words, the mean ratings of unpleasant pictures were significantly greater than those of neutral pictures across the treatment group.

fMRI result

During PBO treatment, unpleasant condition relative to neutral U–N contrast revealed greater activations in the visual cortex, dorsal lateral prefrontal cortex (DLPFC), orbitofrontal cortex (OFC), parietal cortex, insula, amygdala, thalamus, globus pallidus, and brainstem. During SUL treatment, U–N contrast revealed greater activations in the visual cortex, DLPFC, medial prefrontal cortex (MPFC), OFC, parietal cortex, hippocampus, thalamus, caudate body, and brainstem. During FUL treatment, U–N contrast revealed greater activations in the visual cortex,

Table 1
Brain activation in unpleasant condition relative to neutral condition during PBO, SUL, and FLU treatment

Brain region	Coordinates			BA	*Z* score	*t* value	Voxels
PBO							
R. visual cortex (LG, Cu, MOG, IOG, FG, MTG)	48	−66	−5	17, 18, 19, 37, 39	5.76	14	5404
L. visual cortex (LG, Cu, MOG, IOG, FG, MTG)	−44	−80	−3	17, 18, 19, 37, 39	5.29	11.02	
R. DLPFC (MFG, IFG)	46	15	32	9	4.53	7.65	331
L. DLPFC (IFG)	−51	7	33	9	3.82	5.5	53
R. OFC (IFG)	38	26	−18	47	3.49	4.73	59
R. OFC (IFG)	48	19	−8	47	3.27	4.27	27
L. OFC (IFG)	−36	17	−13	47	3.24	4.22	18
R. parietal cortex	30	−58	49	7	4.1	6.28	44
L. insula	−40	9	−6	13	3.36	4.47	31
R. amygdala	18	−3	−15		3.77	5.38	48
L. amygdala	−10	−1	−17		4.03	6.07	104
R. thalamus, GP	14	−2	7		3.71	5.24	66
L. thalamus, GP	−10	2	4		3.95	5.86	78
Brainstem	−4	−33	−2		4.78	8.61	356
SUL							
R. visual cortex (LG, Cu, MOG, IOG, FG)	26	−90	−4	17, 18, 19, 37	4.25	6.71	1109
L. visual cortex (LG, Cu, MOG, IOG, FG)	−28	−91	12	17, 18, 19, 37	4.97	9.45	1537
R. DLPFC (MFG, IFG)	50	26	15	8, 9, 46	4.17	6.47	673
L. DLPFC (IFG)	−48	17	23	9	4.04	6.1	377
MPFC (SFG, MFG, CG)	−2	31	41	8, 32	3.96	5.89	286
MPFC (SFG, MFG,)	−2	50	27	9	3.7	5.22	37
L. OFC (IFG)	−38	15	−11	47	3.48	4.7	45
R. OFC (MFG, IFG)	26	30	−18	11, 47	3.84	5.56	156
R. parietal cortex	32	−60	51	7	3.64	5.07	40
L. hippocampus, PHG	−28	−20	−7	27	4.28	6.82	94
R. thalamus	8	−19	8		4.26	6.76	732
L. thalamus, caudate body	−6	−17	6		4.16	6.44	
Brainstem	−2	−29	−5		4.15	6.42	
FLU							
R. visual cortex (LG, MOG, IOG, FG)	44	−71	−13	18, 19, 37	4.61	7.96	1623
L. visual cortex (LG, Cu, MOG, IOG, FG, ITG)	−38	−86	−4	17, 18, 19, 37	5.33	11.28	2154
R. DLPFC (MFG, IFG)	51	19	34	8, 9	4.44	7.34	323
R. DLPFC (IFG)	48	30	13	46	3.63	5.05	43
L. DLPFC (MFG, IFG)	−44	9	27	9, 46	4.05	6.12	273
R. parietal cortex	18	−73	48	7	3.95	5.84	43
R. parietal cortex	30	−56	49	7	3.86	5.62	123
L. parietal cortex	−30	−57	54	7	4.08	6.2	90
R. thalamus	10	−15	12		3.65	5.1	33
L. thalamus, caudate body	−10	−17	12		3.75	5.34	99
R. GP	14	2	4		3.58	4.93	48
Brainstem	−6	−28	−19		4.25	6.73	28

Significant differences were recognized at a height threshold ($P < 0.001$, uncorrected) and extent threshold (10 voxels). Coordinates and *Z* score refer to the peak of each brain region. BA = Brodmann area; L = left; R = right; LG = lingual gyrus; Cu = cuneus; MOG = middle occipital gyrus; IOG = inferior occipital gyrus; FG = fusiform gyrus; STG = superior temporal gyrus; MTG = middle temporal gyrus; ITG = inferior temporal gyrus; SFG = superior frontal gyrus; MFG = medial frontal gyrus; IFG = inferior frontal gyrus; CG = cingulate gyrus; AC = anterior cingulate; DLPFC = dorsal lateral prefrontal cortex; MPFC = medial prefrontal cortex; OFC = orbitofrontal cortex; GP = globus pallidus.

DLPFC, parietal cortex, thalamus, caudate body, globus pallidus, and brainstem (Table 1 and Fig. 1). Compared to PBO, SUL treatment decreased responses of U–N contrast in the visual cortex, left temporal cortex, anterior cingulate, left amygdaloid–hippocampal region, cerebellum, and midbrain, whereas SUL treatment produced greater activation in the frontal cortex including DLPFC, MPFC, temporal cortex, parietal cortex, left insula, and left claustrum (Table 2 and Fig. 2). On the other hand, compared to PBO, FLU treatment decreased responses of U–N condition in the left OFC, right temporal cortex, right insula, right hippocampal region and left amygdaloid–hippocampal region, and right putamen, whereas FUL treatment produced greater activation in the temporal cortex and parietal cortex (Table 3 and Fig. 3).

During both SUL and FLU treatments, mean signal changes elicited by unpleasant condition compared to neutral condition were significantly less than those during PBO treatment ($t = 2.63$, $P = 0.02$ and $t = 2.93$, $P = 0.01$, respectively) in the left amygdala, but not the right amygdala ($t = 0.57$, $P = 0.57$ and $t = 1.93$, $P = 0.07$, respectively). The differences in mean signal changes between SUL and PBO were 0.36 (95% CI, 0.08–0.65) in the left amygdala and 0.07 (95% CI, −0.18–0.32) in the right amygdala. The differences in mean signal changes between FLU and PBO were 0.24 (95% CI, 0.07–0.41) in the left amygdala and 0.25 (95% CI, −0.17–0.52) in the right amygdala (Fig. 4).

Discussion

We found that acute administration of a therapeutic dose of DA D_2 antagonists and SSRIs had modulatory effects on emotional processing in the human brain, although the subjects recruited the entire neural network of the limbic–cortical–striatal–pallidal–thalamic circuit in response to unpleasant pictures while taking PBO. Our findings indicate that both acute SUL and FLU treatments manipulated the responses of the components of the circuit and commonly attenuated the activation of amygdala, a key node of the circuit.

DA D_2 receptor antagonist treatment decreased responses in the limbic areas (amygdala, hippocampus, anterior cingulate) along with the visual sensory cortex, cerebellum, and midbrain. Not

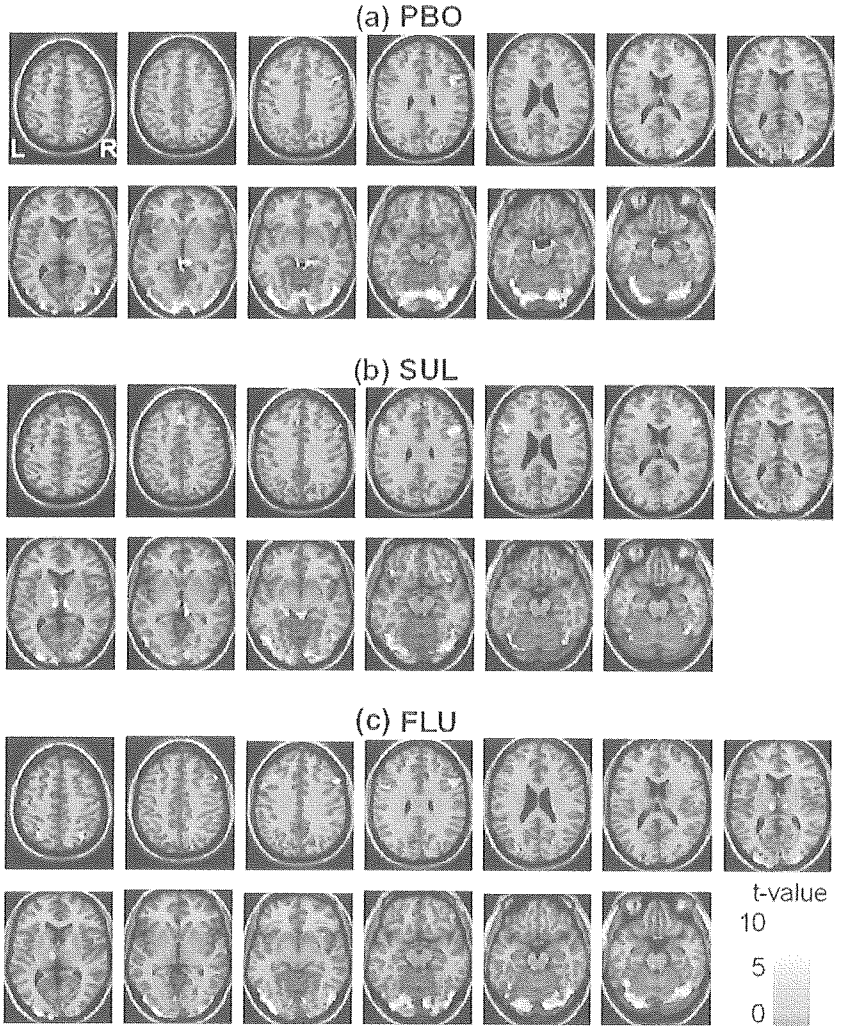

Fig. 1. Images showing dissociable brain activations in unpleasant condition relative to neutral condition during PBO treatment (a), SUL treatment (b), and FLU treatment (c). Significant differences were recognized at a height threshold ($t > 3.93$; $P < 0.001$, uncorrected) and extent threshold (10 voxels). The bar shows the range of the t value. Within the images, L indicates left and R indicates right.

Table 2
Brain regions showing significant effects of SUL treatment on neural activations in response to unpleasant condition relative to neutral condition

Brain region	Coordinates			BA	Z score	t value	Voxels
	x	y	z				
PBO vs. SUL							
L. occipital cortex (LG), cerebellum	−14	−72	−8	18	3.25	4.24	201
L. occipital cortex (Cu)	0	−62	5	30	3.43	4.6	33
L. occipital cortex (Cu)	−8	−78	33	19	3.34	4.42	13
L. occipital cortex (Cu)	−8	−70	16	31	2.96	3.69	12
L. occipital cortex (IOG)	−48	−78	−4	18	3.28	4.29	20
R. occipital cortex (Cu)	20	−92	30	19	2.96	3.7	10
L. temporal cortex (STG)	−34	16	−32	38	3.2	4.13	19
R. AC	2	34	22	32	3.18	4.1	11
L. PHG	−32	−30	−22	36	3.39	4.53	10
L. amygdala	−14	−2	−26		2.91	3.61	10
Midbrain	−10	−12	−15		3.38	4.5	19
SUL vs. PBO							
R. DLPFC (IFG)	55	30	8	46	3.19	4.12	24
L. DLPFC (MFG)	−53	17	25	9	2.88	3.55	14
L. DLPFC (IFG)	−50	5	27	9	3.01	3.77	22
MPFC (MFG)	8	29	45	8	3.17	4.08	29
R. frontal cortex	6	−32	55	4,5	2.96	3.69	46
R. frontal cortex (MFG)	26	−7	48	6	3.69	5.19	137
R. frontal cortex (MFG)	38	46	−6	10	3.17	4.08	35
R. frontal cortex (IFG)	46	22	15	45	3.79	5.44	50
L. frontal cortex (IFG)	−53	22	4	45	3.16	4.07	25
R. temporal cortex (MTG)	55	−49	−3	37	3.63	5.06	15
R. temporal cortex (MTG)	50	−33	0	21	3.16	4.06	53
L. temporal cortex (STG)	−51	−31	3	22	3.48	4.7	48
L. temporal cortex (MTG)	−55	−6	−13	21	3.25	4.24	21
R. parietal cortex	42	−47	41	40	3.62	5.03	88
R. parietal cortex	42	−30	55	40	3.15	4.04	23
R. parietal cortex	50	−13	47	3	3	3.76	19
L. parietal cortex	−38	−32	53	40	2.99	3.75	22
L. parietal cortex	−30	−42	48	40	2.97	3.71	10
L. insula	−48	−9	15	13	3.24	4.22	58
L. claustrum	−38	−25	0		3.27	4.28	93

To compare the effect of SUL on the U−N contrast, paired *t* tests (PBO vs. SUL and SUL vs. PBO) were conducted. Significant differences were recognized at a height threshold ($P < 0.005$, uncorrected) and extent threshold (10 voxels). See Table 1 legend.

surprisingly, attenuation of amygdala response by DA D_2 antagonists was in contrast to the previous pharmacological fMRI study where pharmacotherapy such as levodopa or DA agonists restored the amygdala activation in PD patients (Tessitore et al., 2002). However, the mechanisms underlying these results are not straightforward since DA could potentiate both the excitatory and inhibitory influences of afferent inputs on target neurons (Cohen et al., 2002).

Our PET study demonstrated that DA D_2 receptors are relatively dense in the mesocorticolimbic regions (amygdala, hippocampus, thalamus, and anterior cingulate), besides the striatal regions (Okubo et al., 1999). Considering the regional distributions of DA D_2 receptors, decreased activations in the amygdala, hippocampus, and anterior cingulate by DA D_2 receptor blockade indicate that the net effect of DA D_2 receptor activation is to enhance excitability of limbic regions in response to unpleasant stimuli, although we did not observe significant change of activation in the thalamus and striatal regions.

On the contrary, DA D_2 receptor blockade produced greater activations extensively in the cortical areas (frontal, temporal, and parietal). These enhanced activations in cortical areas are quite puzzling. A possible explanation is that SUL acute treatment might have increased dopaminergic transmission in the cortical area. DA D_2 antagonists are known to increase activity of A9 and A10 neurons through the feedback mechanism of presynaptic D_2-like autoreceptors (Westerink, 2002). Another substituted benzamide derivative, amisulpride, has been suggested to enhance cortical dopaminergic transmission through its preferential blockade of presynaptic D_2-like autoreceptors at optimal dose (Moller, 2003). We revealed that the registered clinical dose of SUL (300–600 mg, max 1800 mg) was about ten times higher than the estimated optimal dose by PET (unpublished data). Thus, if we used SUL at the optimal dose, it would act like amisulpride to enhance cortical dopaminergic transmission in the cortical regions.

Among the enhanced cortical areas, greater activations in the PFC are noteworthy since it is considered to be a main modulator in the neural circuit of emotional processing (Davidson et al., 2002; Drevets, 2000). There are direct and indirect connections between the amygdala and PFC (Groenewegen and Uylings, 2000; Price et al., 1996), and the PFC can attenuate amygdala activation via these connections (Hariri et al., 2000; Rosenkranz and Grace, 1999, 2001). Cognitive demands such as explicit and elaborate evaluation of stimuli that are mediated in the PFC are known to attenuate automatic amygdala activation (Hariri et al., 2000; Phan et al., 2002). In this sense, passive viewing is the ideal way to examine robust amygdala activation, but the behavioral data during the scans should be recorded. To reconcile this dilemma, we used the current paradigm, in which the participants roughly reported their subjective experience, aiming to ensure minimal cognitive demands. Since cognitive demands across the 3 sessions were identical in this design, we can rule out the effect of cognitive demands when interpreting the attenuated amygdala activation, but it remains possible that attenuated amygdala activity is partially attributable to secondary change to the principal drug effect on the PFC. However, since we observed the net effects of direct drug effect on the amygdala and possible secondary modulation by afferent input in the amygdala, we cannot differentiate between these possible mechanisms in this study.

SSRI treatment also decreased the activation in amygdaloid–hippocampal regions, as we predicted. However, unlike DA D_2 receptor antagonists, SSRI treatment reduced activation in different areas such as OFC, basal ganglia, and insula but not in the visual cortex. Moreover, SSRI treatment produced greater activation only in the temporal cortex and parietal cortex, not in the frontal cortex. Although both DA D_2 antagonist and SSRI treatment resulted in common inhibitory effects on activations of amygdaloid–hippocampal regions, the different patterns observed in other regions strongly point to different mechanisms underlying the common effects.

FLU was approved for the treatment of obsessive-compulsive disorder (OCD) but has not been officially approved for the treatment of depression in the United States. However, it is approved in many countries for the indication of depression (Hachisu and Ichimaru, 2000). It is probably no less effective than the other SSRIs in treating depression (Dalery and Honig, 2003) and no better than the other SSRIs at treating OCD (Mundo et al., 1997). FLU has greater selectivity for 5-HT vs. noradrenaline (NA) than fluoxetine and paroxetine and less selectivity than citolopram and sertraline (Wong and Bymaster, 2002). A microdialysis study

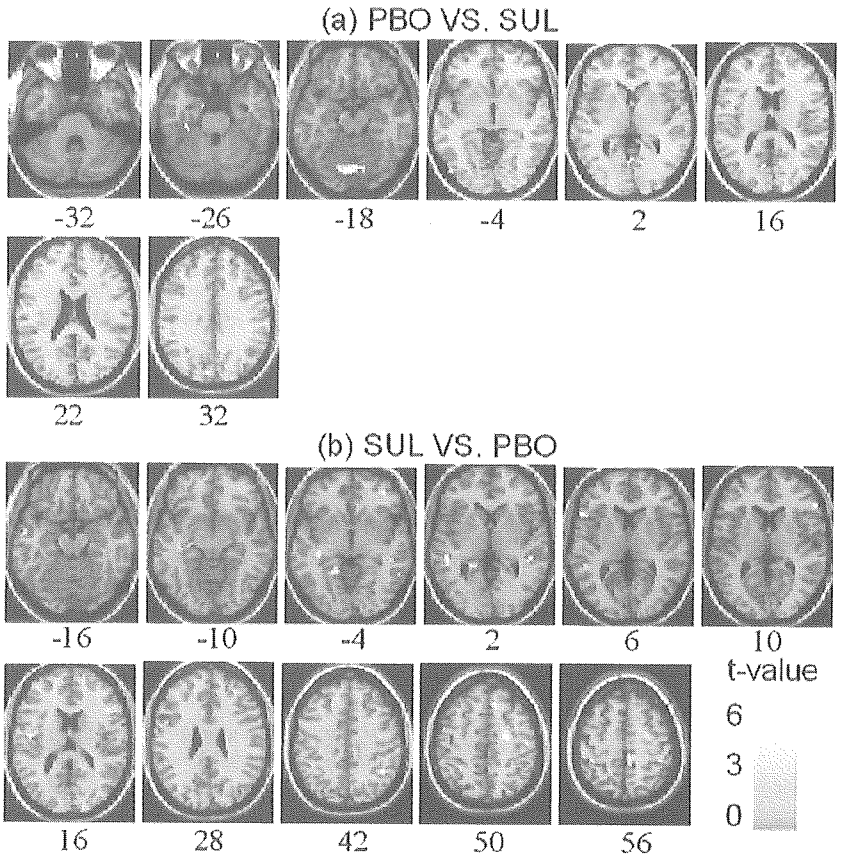

Fig. 2. Images showing manipulated brain activations in response to unpleasant condition relative to neutral condition under SUL treatment. Compared to PBO, attenuated activations were shown in the visual cortex, left temporal cortex, anterior cingulate, left amygdaloid–hippocampal region, cerebellum, and midbrain (a). Enhanced activations were found in the frontal cortex, temporal cortex, parietal cortex, left insula, and left claustrum (b). Significant differences were recognized at a height threshold ($t > 3.05$; $P < 0.005$, uncorrected) and extent threshold (10 voxels). The bar shows the range of the t value. Within the image, L indicates left and R indicates right. Numbers in the bottom row indicate the z coordinates of the Montreal Neurological Institute brain.

demonstrated that SSRIs (FLU, citalopram, sertraline, and paroxetine) did not increase NA and DA extracellular levels in the PFC, and only acute administration of fluoxetine, which has modest selectivity for 5-HT vs. NA compared with other SSRIs, increased them (Bymaster et al., 2002). Therefore, when FLU was administered acutely, the potential effect on the NA or DA system might be negligible in this study.

We understand that the effects of acute SSRI treatment on 5-HT neurotransmission are complex due to the presence of autoreceptors on the presynaptic neuron. The distribution of 5-HT transporters closely matches the regional distribution of 5-HT nerve terminal and cell bodies. They are highly expressed in the amygdala, hippocampus, thalamus, striatum, and midbrain. Intermediate density is found in the cortex and cerebellum (Parsey et al., 2000). Blockade of 5-HT transporters by acute SSRI administration preferentially increases extracellular 5-HT in the raphe nuclei. An increase in somatodendric extracellular 5-HT activates 5-HT_{1A} autoreceptor feedback system to inhibit 5-HT release in terminal projection regions (Pineyro and Blier, 1999). However, preclinical microdialysis studies have consistently reported that acute systemic administration of SSRIs increased extracellular 5-HT concentrations in the raphe nuclei, frontal cortex, hippocampus, and amygdala (Bosker et al., 1995, 2001; Dawson and Nguyen, 1998; Hatanaka et al., 2000; Invernizzi et al., 1995; Malagie et al., 1995). In the present study, acute SSRI administration might have increased 5-HT neurotransmission at postsynaptic 5-HT receptors in the amygdaloid–hippocampal regions because postsynaptic 5-HT receptors are rich in the amygdala and hippocampus (Buhot, 1997; Pineyro and Blier, 1999) and an increase of 5-HT reduced reactivity of the amygdala to sensory inputs (Stutzmann et al., 1998). There are several 5-HT receptor subtypes expressed in the amygdala, and there are both inhibitory (e.g. 5-HT_{1A}) and excitatory (e.g. $5\text{-HT}_{2A}/5\text{-HT}_{2C}$) receptors (Stein et al., 2000). In addition, because excitatory and inhibitory neurons are tightly interconnected in the local circuits, it is unlikely that a large increase in inhibition can be observed without a concomitant increase in excitation. Therefore, we cannot differentiate specific 5-HT receptor subtype effects in this study and what we observed here was the net effect of 5-HT transmission change on the amygdala.

Although the putative anxiolytic and antidepressant effect of SSRIs is generally understood to be associated with a net increase in 5-HT neurotransmission, there are conflicting results on the function of 5-HT in anxiety. Several animal studies in the literature have demonstrated that high 5-HT was associated with anxiety, indicating a major role of 5-HT in the amygdala in the generation of anxiogenic behaviors (Chaouloff, 2000; Graeff et al., 1996). On the other hand, the fact that the success of the treatment with SSRIs and acute tryptophan depletion worsens depressive symptoms in depression suggests that an increase in 5-HT transmission may be

Table 3
Brain regions showing significant effects of FLU treatment on neural activations in response to unpleasant condition relative to neutral condition

Brain region	Coordinates			BA	Z score	t value	Voxels
	x	y	z				
PBO vs. FLU							
L. OFC (IFG)	−32	26	−15	47	3.05	3.85	16
R. temporal cortex (STG)	63	−34	11	22	3.8	5.47	52
R. insula	48	1	10	13	3.45	4.64	27
R. PHG	22	−17	−21	28	3.28	4.29	29
R. hippocampus	26	−11	−16		3.5	4.75	35
L. amygdala, hippocampus	−24	−12	−11		3.6	4.99	84
R. putamen	28	−2	−3		2.91	3.61	13
FLU vs. PBO							
R. temporal cortex (MTG)	59	−47	−8	37	3.49	4.74	49
R. temporal cortex (MTG)	55	−29	−5	21	3.08	3.92	46
R. temporal cortex (STG)	48	−18	−6	22	3.14	4.02	17
L. temporal cortex (STG, MTG)	−51	−39	6	22	3.2	4.14	31
L. parietal cortex	−24	−72	39	7	3.84	5.57	62
L. parietal cortex	−46	−32	51	40	3.32	4.38	44

To compare the effect of FLU on the U–N contrast, paired t tests (PBO vs. FLU and FUL vs. PBO) were conducted. Significant differences were recognized at a height threshold ($P < 0.005$, uncorrected) and extent threshold (10 voxels). See Table 1 legend.

anxiolytic in humans (Kent et al., 1998). Preclinical studies reported that emotional stress increases 5-HT concentration in the amygdala and prefrontal cortex (Amat et al., 2005; Kawahara et al., 1993), and an increase of 5-HT reduces reactivity of the amygdala to excitatory sensory inputs (Stutzmann et al., 1998). This has led to the suggestion that 5-HT may act as a constraint system to inhibit primitive and impulsive reaction by reducing responsiveness of lower brain centers to emotional stress (Kent et al., 1998; Spoont, 1992). Stress from viewing unpleasant pictures might have increased endogenous 5-HT release, and SSRI might have potentiated 5-HT function to reduce reactivity of the amygdala in this study.

Interestingly, the effects of both SUL and FUL on the amygdala treatment were lateralized to the left side. It has been suggested regarding the functional laterality of the amygdala that the right amygdala may be first activated by emotional stimuli and be engaged in a rapid automatic processing of ambiguous information, while the left amygdala may be involved in a more specific sustained emotional reaction that decodes the arousal signaled by specific stimuli (Glascher and Adolphs, 2003). The reduced activity of the left amygdala might reflect reduction of the arousal. Since we used a rough self-rating score of unpleasantness, we did not have variations in terms of unpleasantness. If we had used a more detailed self-rating score of unpleasantness, the score might have detected the reduction of subjective unpleasantness. In addition, in terms of FLU treatment, it is perhaps worth remarking that, although the differences in mean signal changes elicited by unpleasant conditions compared to neutral condition in both left and right amygdala were similar, the right amygdala failed to reach a level of significance due to the greater variations in terms of the effect of SSRI treatment. Recent studies revealed that genetic variations of 5-HT transporters are associated with individual differences of right amygdala activity (Hariri et al., 2002b, 2005). Variations in the effect of SSRI treatment on the right amygdala could be attributable to genetic variations of 5-HT transporters.

Chronic successful treatments with SSRIs that normalized the elevated amygdala activity in patients with depression have been reported (Drevets, 2000). Since the therapeutic effect of SSRIs can take several weeks to appear, the mechanisms underlying the therapeutic effect of their chronic treatment are considered to be different from those of the acute pharmacological change induced by acute SSRI administration. However, our data suggest that even acute treatment of SSRIs could produce desirable preclinical

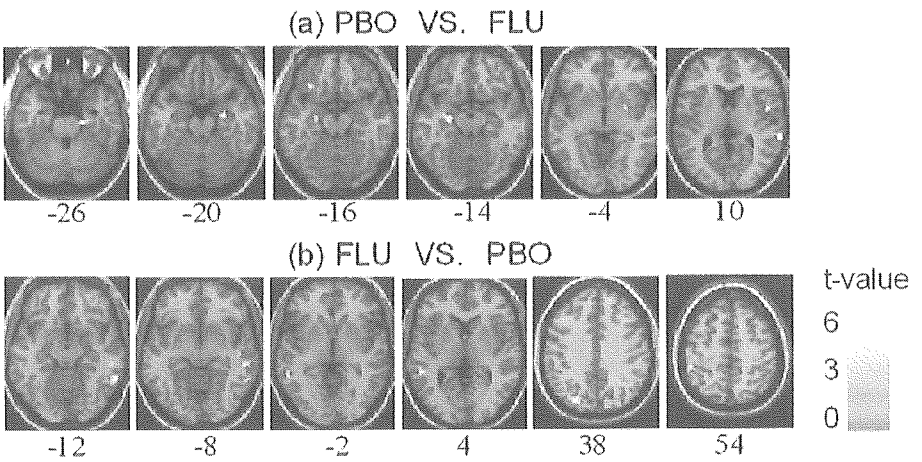

Fig. 3. Images showing manipulated brain activations in response to unpleasant condition relative to neutral condition under FLU treatment. Compared to PBO, attenuated activations were shown in the left OFC, right temporal cortex, right insula, right hippocampal region, left amygdaloid–hippocampal region, and right putamen (a). Enhanced activations were found in the temporal cortex and parietal cortex (b). Significant differences were recognized at a height threshold ($t > 3.05$; $P < 0.005$, uncorrected) and extent threshold (10 voxels). The bar shows the range of the t value. Within the image, L indicates left and R indicates right. Numbers in the bottom row indicate the z coordinates of the Montreal Neurological Institute brain.

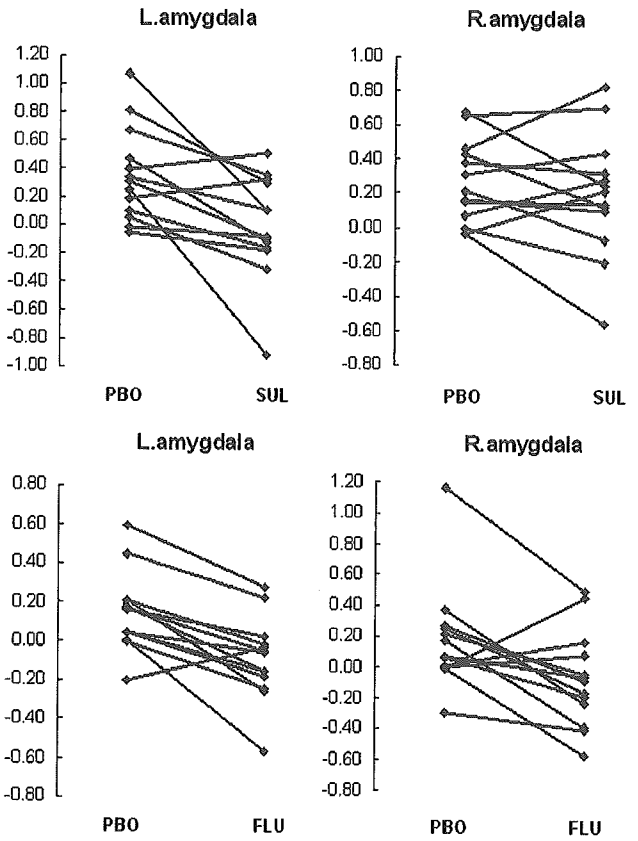

Fig. 4. Individual differences in the effect of drugs on amygdala activation elicited by unpleasant condition compared to neutral condition. The effect of sultopride on the left amygdala ($x, y, z = -14, -3, -22$) and the right amygdala ($x, y, z = 22, -3, -15$) (top). The effect of fluvoxamine on the left amygdala ($x, y, z = -24, -12, -11$) and the right amygdala ($x, y, z = 26, 1, -22$) (bottom). During both drugs treatments, mean signal changes elicited by unpleasant condition compared to neutral condition were significantly less than those during placebo treatment ($t = 2.63$, $P = 0.02$ and $t = 2.93$, $P = 0.01$, respectively) in the left amygdala, but not in the right amygdala ($t = 0.57$, $P = 0.57$ and $t = 1.93$, $P = 0.07$, respectively).

physiological changes, i.e., normalization of abnormally elevated amygdala activity, in patients with depression or anxiety disorders.

The present study has several limitations. First, it is possible that the drugs have effects not only on the specific neuronal activation but also on nonspecific vascular and respiratory systems that could, in turn, change BOLD signals. However, it could be considered that the observed regional BOLD changes mostly reflected the specific effects on neuronal responses because nonspecific effects would produce BOLD signal changes to a similar degree in any region across the brain (Honey and Bullmore, 2004). Moreover, we believed that nonspecific effects were minimized, if any, because the drugs induced minimal changes of physiological data. Second, we reported the drug effects on BOLD maps without correcting multiple comparisons. This raises the risk of type 1 errors. However, because pharmacological fMRI is a relatively new method and we do not possess sufficient information about the possible drug effects on BOLD signals across the whole brain, determining regions of interest (ROIs) a priori would be difficult. Therefore, we did not correct for multiple comparisons using ROIs.

Third, we examined the effects of DA D_2 receptor antagonists and SSRIs in healthy volunteers in this study. These drugs might not necessarily show similar actions in patients with psychiatric disorders, such as schizophrenia, mood disorders, and anxiety disorders. Studies on drug-free psychiatric disorder patients should be performed. Finally, despite significant changes of neural activation by pharmacological manipulation, behavioral results did not show significant changes. We had the subjects rate the pictures roughly using a 3-point scale. We aimed to simplify the emotional task and reduce cognitive demands during the scan since cognitive demands such as detailed evaluation or pressing several buttons could attenuate automatic emotional responses (Phan et al., 2002). Although this rough measurement might be attributable to insensitivity, conventional behavioral measurements are considered not sensitive enough to detect drugs effects (Honey and Bullmore, 2004).

In conclusion, we have shown that acute treatments of DA D_2 receptor antagonists and SSRIs commonly achieved considerable attenuation of amygdala activity, although the two treatments had different modulatory effects on other components of the neural circuit of emotional processing in healthy subjects.

The results suggest that the effects of the drug itself on BOLD signals are likely not negligible in fMRI studies aiming to investigate emotional processing in psychiatric patients taking drugs. At the same time, our findings suggest that pharmacological fMRI might be a powerful measurement tool for investigating the effects of drugs that manipulate neurotransmitter systems on emotional processing in the human brain and that this tool has potential for application in clinical practice and drug discovery.

Acknowledgments

The staffs of the Section of Biofunctional Informatics, Graduate School of Medicine, Tokyo Medical and Dental University, and of Asai Hospital are gratefully acknowledged. This work was supported by a Grant-in-Aid for Scientific Research from the Japanese Ministry of Education, Culture, Sports, Science and Technology (15390438), a research grant for nervous and mental disorders (14B-3), and a Health and Labor Sciences Research Grant for Research on Psychiatric and Neurological Diseases and Mental Health (H15-KOKORO-003) from the Japanese Ministry of Health, Labor and Welfare. NY acknowledges the support from the Japan Foundation for Aging and Health (research resident).

References

Amat, J., Baratta, M.V., Paul, E., Bland, S.T., Watkins, L.R., Maier, S.F., 2005. Medial prefrontal cortex determines how stressor controllability affects behavior and dorsal raphe nucleus. Nat. Neurosci. 8, 365–371.

Bosker, F.J., Klompmakers, A.A., Westenberg, H.G., 1995. Effects of single and repeated oral administration of fluvoxamine on extracellular serotonin in the median raphe nucleus and dorsal hippocampus of the rat. Neuropharmacology 34, 501–508.

Bosker, F.J., Cremers, T.I., Jongsma, M.E., Westerink, B.H., Wikstrom, H.V., den Boer, J.A., 2001. Acute and chronic effects of citalopram on postsynaptic 5-hydroxytryptamine(1A) receptor-mediated feedback: a microdialysis study in the amygdala. J. Neurochem. 76, 1645–1653.

Buhot, M.C., 1997. Serotonin receptors in cognitive behaviors. Curr. Opin. Neurobiol. 7, 243–254.

Bymaster, F.P., Zhang, W., Carter, P.A., Shaw, J., Chernet, E., Phebus, L., Wong, D.T., Perry, K.W., 2002. Fluoxetine, but not other selective serotonin uptake inhibitors, increases norepinephrine and dopamine extracellular levels in prefrontal cortex. Psychopharmacology (Berlin) 160, 353–361.

Cardinal, R.N., Parkinson, J.A., Hall, J., Everitt, B.J., 2002. Emotion and motivation: the role of the amygdala, ventral striatum, and prefrontal cortex. Neurosci. Biobehav. Rev. 26, 321–352.

Chaouloff, F., 2000. Serotonin, stress and corticoids. J. Psychopharmacol. 14, 139–151.

Cohen, J.D., Braver, T.S., Brown, J.W., 2002. Computational perspectives on dopamine function in prefrontal cortex. Curr. Opin. Neurobiol. 12, 223–229.

Dalery, J., Honig, A., 2003. Fluvoxamine versus fluoxetine in major depressive episode: a double-blind randomised comparison. Hum. Psychopharmacol. 18, 379–384.

Davidson, R.J., Lewis, D.A., Alloy, L.B., Amaral, D.G., Bush, G., Cohen, J.D., Drevets, W.C., Farah, M.J., Kagan, J., McClelland, J.L., Nolen-Hoeksema, S., Peterson, B.S., 2002. Neural and behavioral substrates of mood and mood regulation. Biol. Psychiatry 52, 478–502.

Dawson, L.A., Nguyen, H.Q., 1998. Effects of 5-HT1A receptor antagonists on fluoxetine-induced changes in extracellular serotonin concentrations in rat frontal cortex. Eur. J. Pharmacol. 345, 41–46.

DeVane, C.L., Gill, H.S., 1997. Clinical pharmacokinetics of fluvoxamine: applications to dosage regimen design. J. Clin. Psychiatry 58 (Suppl. 5), 7–14.

Drevets, W.C., 2000. Neuroimaging studies of mood disorders. Biol. Psychiatry 48, 813–829.

Farde, L., Nordstrom, A.L., Wiesel, F.A., Pauli, S., Halldin, C., Sedvall, G., 1992. Positron emission tomographic analysis of central D1 and D2 dopamine receptor occupancy in patients treated with classical neuroleptics and clozapine. Relation to extrapyramidal side effects. Arch. Gen. Psychiatry 49, 538–544.

Glascher, J., Adolphs, R., 2003. Processing of the arousal of subliminal and supraliminal emotional stimuli by the human amygdala. J. Neurosci. 23, 10274–10282.

Graeff, F.G., Guimaraes, F.S., De Andrade, T.G., Deakin, J.F., 1996. Role of 5-HT in stress, anxiety, and depression. Pharmacol. Biochem. Behav. 54, 129–141.

Groenewegen, H.J., Uylings, H.B., 2000. The prefrontal cortex and the integration of sensory, limbic and autonomic information. Prog. Brain Res. 126, 3–28.

Hachisu, M., Ichimaru, Y., 2000. Pharmacological and clinical aspects of fluvoxamine (Depromel), the first selective serotonin reuptake inhibitor approved for clinical use employed in Japan. Nippon Yakurigaku Zasshi 115, 271–279.

Hariri, A.R., Bookheimer, S.Y., Mazziotta, J.C., 2000. Modulating emotional responses: effects of a neocortical network on the limbic system. NeuroReport 11, 43–48.

Hariri, A.R., Mattay, V.S., Tessitore, A., Fera, F., Smith, W.G., Weinberger, D.R., 2002a. Dextroamphetamine modulates the response of the human amygdala. Neuropsychopharmacology 27, 1036–1040.

Hariri, A.R., Mattay, V.S., Tessitore, A., Kolachana, B., Fera, F., Goldman, D., Egan, M.F., Weinberger, D.R., 2002b. Serotonin transporter genetic variation and the response of the human amygdala. Science 297, 400–403.

Hariri, A.R., Drabant, E.M., Munoz, K.E., Kolachana, B.S., Mattay, V.S., Egan, M.F., Weinberger, D.R., Tessitore, A., Kolachana, B., Fera, F., Goldman, D., 2005. A susceptibility gene for affective disorders and the response of the human amygdala. Arch. Gen. Psychiatry 62, 146–152.

Harmer, C.J., Bhagwagar, Z., Perrett, D.I., Vollm, B.A., Cowen, P.J., Goodwin, G.M., 2003a. Acute SSRI administration affects the processing of social cues in healthy volunteers. Neuropsychopharmacology 28, 148–152.

Harmer, C.J., Hill, S.A., Taylor, M.J., Cowen, P.J., Goodwin, G.M., 2003b. Toward a neuropsychological theory of antidepressant drug action: increase in positive emotional bias after potentiation of norepinephrine activity. Am. J. Psychiatry 160, 990–992.

Hatanaka, K., Yatsugi, S., Yamaguchi, T., 2000. Effect of acute treatment with YM992 on extracellular serotonin levels in the rat frontal cortex. Eur. J. Pharmacol. 395, 23–29.

Honey, G., Bullmore, E., 2004. Human pharmacological MRI. Trends Pharmacol. Sci. 25, 366–374.

Invernizzi, R., Bramante, M., Samanin, R., 1995. Extracellular concentrations of serotonin in the dorsal hippocampus after acute and chronic treatment with citalopram. Brain Res. 696, 62–66.

Kapur, S., Zipursky, R., Jones, C., Remington, G., Houle, S., 2000. Relationship between dopamine D(2) occupancy, clinical response, and side effects: a double-blind PET study of first-episode schizophrenia. Am. J. Psychiatry 157, 514–520.

Kapur, S., Langlois, X., Vinken, P., Megens, A.A., De Coster, R., Andrews, J.S., 2002. The differential effects of atypical antipsychotics on prolactin elevation are explained by their differential blood–brain disposition: a pharmacological analysis in rats. J. Pharmacol. Exp. Ther. 302, 1129–1134.

Kawahara, H., Yoshida, M., Yokoo, H., Nishi, M., Tanaka, M., 1993. Psychological stress increases serotonin release in the rat amygdala and prefrontal cortex assessed by in vivo microdialysis. Neurosci. Lett. 162, 81–84.

Kemp, A.H., Gray, M.A., Silberstein, R.B., Armstrong, S.M., Nathan, P.J., 2004. Augmentation of serotonin enhances pleasant and suppresses unpleasant cortical electrophysiological responses to visual emotional stimuli in humans. NeuroImage 22, 1084–1096.

Kent, J.M., Rauch, S.L., 2003. Neurocircuitry of anxiety disorders. Curr. Psychiatry Rep. 5, 266–273.

Kent, J.M., Coplan, J.D., Gorman, J.M., 1998. Clinical utility of the selective serotonin reuptake inhibitors in the spectrum of anxiety. Biol. Psychiatry 44, 812–824.

Kobari, T., Iguro, Y., Ito, T., Namekawa, H., Kato, Y., Yamada, S., 1985. Absorption, distribution and excretion of sultopride in man and several animal species. Xenobiotica 15, 605–613.

Lang, P.J., Bradley, M.M., Cuthbert, B.N., 1997. International Affective Picture System (IAPS): Technical Manual and Affective Ratings. Center for Research in Psychophysiology, University of Florida, Gainesville.

Malagie, I., Trillat, A.C., Jacquot, C., Gardier, A.M., 1995. Effects of acute fluoxetine on extracellular serotonin levels in the raphe: an in vivo microdialysis study. Eur. J. Pharmacol. 286, 213–217.

Mehta, M.A., Hinton, E.C., Montgomery, A.J., Bantick, R.A., Grasby, P.M., 2005. Sulpiride and mnemonic function: effects of a dopamine D2 receptor antagonist on working memory, emotional memory and long-term memory in healthy volunteers. J. Psychopharmacol. 19, 29–38.

Mizuchi, A., Kitagawa, N., Miyachi, Y., 1983. Regional distribution of sultopride and sulpiride in rat brain measured by radioimmunoassay. Psychopharmacology (Berlin) 81, 195–198.

Moller, H.J., 2003. Amisulpride: limbic specificity and the mechanism of antipsychotic atypicality. Prog. Neuro-Psychopharmacol. Biol. Psychiatry 27, 1101–1111.

Mundo, E., Bianchi, L., Bellodi, L., 1997. Efficacy of fluvoxamine, paroxetine, and citalopram in the treatment of obsessive-compulsive disorder: a single-blind study. J. Clin. Psychopharmacol. 17, 267–271.

Okubo, Y., Olsson, H., Ito, H., Lofti, M., Suhara, T., Halldin, C., Farde, L., 1999. PET mapping of extrastriatal D2-like dopamine receptors in the human brain using an anatomic standardization technique and [11C] FLB 457. NeuroImage 10, 666–674.

Paradiso, S., Andreasen, N.C., Crespo-Facorro, B., O'Leary, D.S., Watkins, G.L., Boles Ponto, L.L., Hichwa, R.D., 2003. Emotions in unmedicated patients with schizophrenia during evaluation with positron emission tomography. Am. J. Psychiatry 160, 1775–1783.

Parsey, R.V., Kegeles, L.S., Hwang, D.R., Simpson, N., Abi-Dargham, A., Mawlawi, O., Slifstein, M., Van Heertum, R.L., Mann, J.J., Laruelle, M., 2000. In vivo quantification of brain serotonin transporters in humans using [11C]McN 5652. J. Nucl. Med. 41, 1465–1477.

Phan, K.L., Wager, T., Taylor, S.F., Liberzon, I., 2002. Functional neuroanatomy of emotion: a meta-analysis of emotion activation studies in PET and fMRI. NeuroImage 16, 331–348.

Pineyro, G., Blier, P., 1999. Autoregulation of serotonin neurons: role in antidepressant drug action. Pharmacol. Rev. 51, 533–591.

Posternak, M.A., Zimmerman, M., 2005. Is there a delay in the antidepressant effect? A meta-analysis. J. Clin. Psychiatry 66, 148–158.

Pralong, E., Magistretti, P., Stoop, R., 2002. Cellular perspectives on the glutamate–monoamine interactions in limbic lobe structures and their relevance for some psychiatric disorders. Prog. Neurobiol. 67, 173–202.

Price, J.L., Carmichael, S.T., Drevets, W.C., 1996. Networks related to the orbital and medial prefrontal cortex; a substrate for emotional behavior? Prog. Brain Res. 107, 523–536.

Rauch, S.L., Shin, L.M., Wright, C.I., 2003. Neuroimaging studies of amygdala function in anxiety disorders. Ann. N. Y. Acad. Sci. 985, 389–410.

Rosenkranz, J.A., Grace, A.A., 1999. Modulation of basolateral amygdala neuronal firing and afferent drive by dopamine receptor activation in vivo. J. Neurosci. 19, 11027–11039.

Rosenkranz, J.A., Grace, A.A., 2001. Dopamine attenuates prefrontal cortical suppression of sensory inputs to the basolateral amygdala of rats. J. Neurosci. 21, 4090–4103.

Spoont, M.R., 1992. Modulatory role of serotonin in neural information processing: implications for human psychopathology. Psychol. Bull. 112, 330–350.

Stein, C., Davidowa, H., Albrecht, D., 2000. 5-HT(1A) receptor-mediated inhibition and 5-HT(2) as well as 5-HT(3) receptor-mediated excitation in different subdivisions of the rat amygdala. Synapse 38, 328–337.

Stutzmann, G.E., McEwen, B.S., LeDoux, J.E., 1998. Serotonin modulation of sensory inputs to the lateral amygdala: dependency on corticosterone. J. Neurosci. 18, 9529–9538.

Suhara, T., Takano, A., Sudo, Y., Ichimiya, T., Inoue, M., Yasuno, F., Ikoma, Y., Okubo, Y., 2003. High levels of serotonin transporter occupancy with low-dose clomipramine in comparative occupancy study with fluvoxamine using positron emission tomography. Arch. Gen. Psychiatry 60, 386–391.

Takahashi, H., Koeda, M., Oda, K., Matsuda, T., Matsushima, E., Matsuura, M., Asai, K., Okubo, Y., 2004. An fMRI study of differential neural response to affective pictures in schizophrenia. NeuroImage 22, 1247–1254.

Talairach, J., Tournoux, P., 1988. Co-planar Stereotaxic Atlas of the Human Brain: Three-dimensional Proportional System. Thieme Medical, New York.

Tessitore, A., Hariri, A.R., Fera, F., Smith, W.G., Chase, T.N., Hyde, T.M., Weinberger, D.R., Mattay, V.S., 2002. Dopamine modulates the response of the human amygdala: a study in Parkinson's disease. J. Neurosci. 22, 9099–9103.

Walczak, D.D., Apter, J.T., Halikas, J.A., Borison, R.L., Carman, J.S., Post, G.L., Patrick, R., Cohn, J.B., Cunningham, L.A., Rittberg, B., Preskorn, S.H., Kang, J.S., Wilcox, C.S., 1996. The oral dose–effect relationship for fluvoxamine: a fixed-dose comparison against placebo in depressed outpatients. Ann. Clin. Psychiatry 8, 139–151.

Westerink, B.H., 2002. Can antipsychotic drugs be classified by their effects on a particular group of dopamine neurons in the brain? Eur. J. Pharmacol. 455, 1–18.

Wong, D.T., Bymaster, F.P., 2002. Dual serotonin and noradrenaline uptake inhibitor class of antidepressants potential for greater efficacy or just hype? Prog. Drug. Res. 58, 169–222.

Available online at www.sciencedirect.com

SCIENCE DIRECT®

Psychiatry Research: Neuroimaging 138 (2005) 197–207

PSYCHIATRY RESEARCH NEUROIMAGING

www.elsevier.com/locate/psychresns

Abnormal effective connectivity of dopamine D2 receptor binding in schizophrenia

Fumihiko Yasuno[a,b], Tetsuya Suhara[a,b,*], Yoshiro Okubo[c], Tetsuya Ichimiya[a,b], Akihiro Takano[a,b], Yasuhiko Sudo[a,b], Makoto Inoue[a,b]

[a]*Brain Imaging Project, National Institute of Radiological Sciences, 4-9-1 Anagawa, Inage-ku, Chiba 263-8555, Japan*
[b]*CREST Japan Science and Technology Corporation, Saitama 332-0012, Japan*
[c]*Department of Psychiatry, Nippon Medical School, 1-1-5 Sendagi, Bunkyo-ku, Tokyo 113-8603, Japan*

Received 30 October 2003; accepted 7 April 2004

Abstract

Receptor binding has been examined region by region in both in vitro and in vivo studies, but less attention has been paid to the connectivity of regional receptor binding despite the fact that neurophysiological studies have indicated an extensive inter-regional connectivity. In this study, we investigated the connectivity of regional dopamine D2 receptor binding in positron emission tomography data from 10 drug-naïve patients with schizophrenia and 19 healthy controls. We applied a structural equation method to regional receptor binding. The results indicated that the network models of the patients and normal subjects were significantly different. As to the individual path coefficients, (a) connectivity between cortical regions was different between groups; (b) connectivity from the prefrontal cortex, parietal cortex, and thalamus to the anterior cingulate differed from that in controls; and (c) connectivity from the prefrontal cortex to the anterior cingulate and thalamus via the hippocampus was observed in normal subjects but not in patients. These results suggest that a systems-level change reflected in the connectivity of D2 receptor binding is present in schizophrenia.
© 2005 Published by Elsevier Ireland Ltd.

Keywords: PET; Structural equation modeling; Dopamine; D2 receptor; Schizophrenia

1. Introduction

A number of morphological and neurochemical abnormalities have been found to characterize schizophrenia. In particular, the dopamine D2 receptor has been investigated extensively, since the chronic use of amphetamine can cause psychotic symptoms and dopamine D2 receptor antagonists are the most widely used drugs for the treatment of schizophrenia. We have recently reported a reduction of dopamine D2 receptor binding in the anterior cingulate of patients with schizophrenia (Suhara et al., 2002). On the other hand, abnormal inter-regional connectivity has been

* Corresponding author. Brain Imaging Project, National Institute of Radiological Sciences, 9-1, Anagawa 4-Chome, Inage-ku, Chiba 263-8555, Japan. Tel.: +81 43 206 3194; fax: +81 43 253 0396.
E-mail address: suhara@nirs.go.jp (T. Suhara).

0925-4927/$ - see front matter © 2005 Published by Elsevier Ireland Ltd.
doi:10.1016/j.pscychresns.2004.04.005

reported in neurophysiological studies of schizophrenia. Interdependence between the different dopaminergic pathways arising in the ventral mesencephalon is a general property of this neuron group (Simon et al., 1988; Louilot et al., 1989). Dopamine systems interact with several other neurotransmitter systems with direct or indirect synaptic connections (Sulzer et al., 1998), and aberrant interactions among different neural networks could lead to an unusual inter-regional dopaminergic tone.

The present study used structural equation modeling to evaluate the connectivity of regional D2 receptor binding in schizophrenia patients and normal controls (McIntosh and Gonzalez-Lima, 1994; McIntosh et al., 1994; Horwitz et al., 1999) in earlier published data (Suhara et al., 2002) and new data from positron emission tomography (PET) and matching magnetic resonance imaging (MRI) (Fig. 1). By this method, the inter-regional correlations of D2 receptor binding were decomposed to assign numerical weights (path coefficients) to the anatomical connections. This computational method allows for the assessment of changes in the inter-regional associations of entire systems. It has been applied to the metabolic mapping data of functional brain imaging in which the model evaluated the influences on a relatively short (within minutes) time scale (Horwitz et al., 1995; Jennings et al., 1998a, b; Della-Maggiore et al., 2000; Goncalves et al., 2001). We applied this method to findings of regional receptor binding that could be assumed to influence each other and to change over the course of illness via the structural neuronal network. The strength and signs of these path coefficients were compared between groups and used to identify disease-specific changes in the connectivity of regional D2 receptor binding within the same anatomical network.

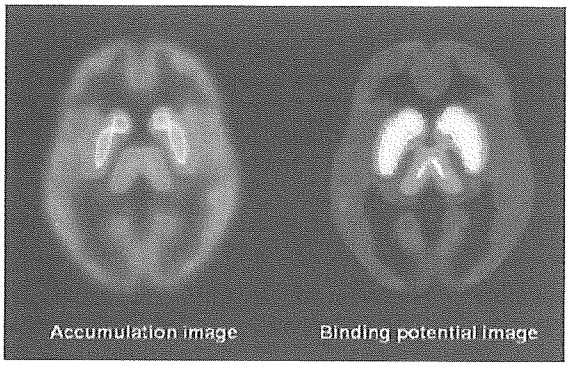

Fig. 1. Images of average accumulation of radioactivity and binding potential (BP) of [^{11}C]FLB 457 in normal controls (n=19). The individual images were anatomically standardized and averaged using Statistical Parametric Mapping (Friston et al., 1995). The images are at a level that includes the thalamus, anterior cingulate and fronto–temporal cortex. Colors show radioactivity and binding potential; red is high and purple is low. We could not evaluate BP in the striatum because of methodological problems and showed it as white blanks in the BP image.

2. Methods

2.1. Subjects

Ten drug-naïve male patients with schizophrenia (mean age=29.5, SD=7.8 years) who met DSM-IV criteria for schizophrenia or schizophreniform disorder were studied. Those with schizophreniform disorder at study entry met the criteria for schizophrenia at 6-month follow-up. Eight of the patients with individual MRI were the same as those reported in the previous study (Suhara et al., 2002), and two were newly recruited for this study with individual MRI. Three patients from the previous study were excluded because of the lack of MR images. The duration of illness ranged from 1 month to 7 years. Brief Psychiatric Rating Scale (BPRS) total scores ranged from 14 to 42 (mean=29.3, SD=8.9), with relatively higher scores for positive symptoms (mean=14.2, SD=4.0) than for negative symptoms (mean=5.5, SD=4.6) (Suhara et al., 2002). The control group comprised 19 age-matched healthy males (mean age=29.6, SD=7.5 years) who did not meet criteria for any neuropsychiatric disorder and who had no relatives with neuropsychiatric disorders. After explanation of the study, written informed consent was obtained from all patients and healthy subjects. This study was approved by the Ethics and Radiation Safety Committee of the National Institute of Radiological Sciences, Chiba, Japan.

2.2. PET and MRI procedures

The ECAT EXACT HR+ (CTI-Siemens, Knoxville, TN, USA) was used to track radioactivity. The

system provides 63 planes and a 15.5-cm field of view (FOV). To minimize head movement, a head fixation device (Fixster, Stockholm, Sweden) was used. A transmission scan for attenuation correction was performed using a ^{68}Ge–^{68}Ga source. Acquisitions were done in a three-dimensional mode with the interplane septa retracted. A bolus of 89.5–249.0 (mean=172.5, SD=40.0) MBq of [^{11}C]FLB 457 with high specific radioactivities (64.9–534.9 GBq/μmol) was injected intravenously into the antecubital vein with a 20-ml saline flush. This ligand was used because its high affinity provided sufficient signal-to-noise ratio in cortical and limbic regions with relatively low dopamine D_2 receptor density. Dynamic scans were performed for 80 min immediately after the injection. All emission scans were reconstructed with a Hanning filter cut-off frequency of 0.4 (full-width half-maximum=7.5 mm). The MR images were acquired on a Phillips Gyroscan NT, and 1.5-Tesla. T1-weighted images of the brain were obtained for all subjects. The scan parameters were 1-mm-thick three-dimensional T1 images with a transverse plane (TR/TE 19/10 ms, flip angle 30°, matrix 256 × 256, FOV 256 mm × 256 mm, NEX 1).

2.3. Quantification of extrastriatal dopamine D2 receptors

Radioactivity in eight brain regions (anterior cingulate, thalamus, hippocampus, prefrontal cortex, temporal cortex and parietal cortex and midbrain/ventral tegmental area) was examined. A subset of these regions has been considered to be related to schizophrenic symptoms (Vollenweider, 1998). In this study we did not evaluate the striatal data because [^{11}C]FLB 457 is not a suitable ligand for quantitative analysis of the striatum (Farde et al., 1997; Suhara et al., 1999). Radioactivity of the cerebellum was also measured for the quantitative analysis. Radioactivity was derived from the mean of the voxel value within both right and left volumes of interest (VOIs) to increase the signal-to-noise ratio for the calculations and to simplify the assumptions and the model concerning the direction of influences and anatomy (Fig. 2).

Regional radioactivity of brain regions was obtained with a template-based method for defining VOIs as described in our recent article (Yasuno et al., 2002), with the exception of the midbrain/ventral

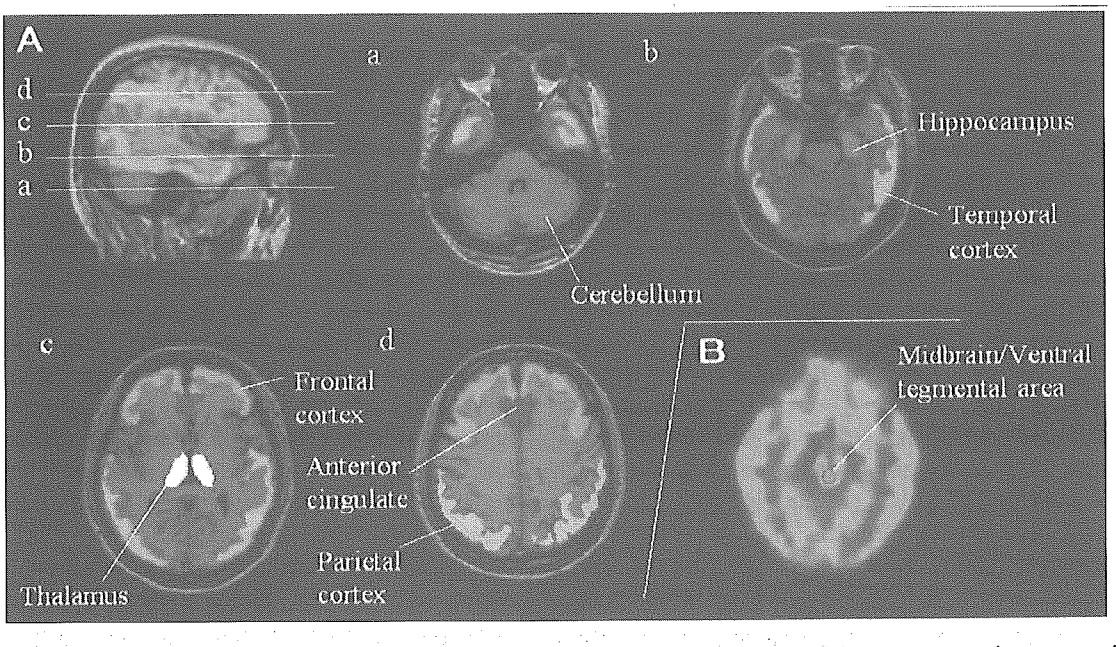

Fig. 2. (a) The transformed VOI template placed on the axial slices of an MRI of one subject after refining to a segmented gray matter image. The horizontal lines through the sagittal section indicate the point of intersection for each of the corresponding axial sections. (b) The manually delineated circular ROI overlying the midbrain area containing the raphe nuclei in the axial plane of summated PET images of one subject.

tegmental area. In short, the template-based method consisted of two major steps. The first step involved the spatial transformation of a template of a VOI from a model MRI to an individual MRI. The second step was to refine the transformed VOI to the individual segmented gray matter of the MRI using the intensity characteristics of these images. The finally refined VOIs were linearly transformed with the parameters obtained from the co-registration of the individual MRIs to PET images. The VOI on the midbrain/ventral tegmental area was defined as follows: a circular region of interest (ROI; 5-mm radius) was centered over the midbrain identified in the co-registered MRI where the ventral tegmental area was evident in the PET summation images.

The volume of the VOI defined on MR images was measured. The sizes of the area were summed across slices and multiplied by slice thickness (1 mm), yielding approximate volumes. The sizes [region (mean ± SD of control vs. patient)] were as follows: prefrontal cortex (16.0 ± 2.8 vs.15.8 ± 2.3 cm^3), temporal cortex (58.4 ± 4.5 vs. 59.9 ± 8.1 cm^3), parietal cortex (30.5 ± 5.1 vs. 28.5 ± 3.9 cm^3), thalamus (8.7 ± 1.6 vs.8.5 ± 1.1 cm^3), hippocampus (5.8 ± 0.8 vs. 5.1 ± 0.7 cm^3), anterior cingulate (4.7 ± 1.0 vs.4.6 ± 0.7 cm^3). The size of the midbrain/ventral tegmental area was the same among subjects (2.4 cm^3).

Quantitative tracer kinetic modeling was performed using a three-parameter (simplified) reference tissue compartmental model (Lammertsma and Hume, 1996). The cerebellum was used as reference tissue because it is nearly devoid of D2 receptors (Farde et al., 1997; Suhara et al., 1999). The model allows the estimation of binding potential (BP), which can be regarded as an index of receptor binding. BP is defined as follows; $BP=f_2B_{max}/\{K_d[1+\Sigma_i F_i/K_{di}]\}$, where f_2 is the "free fraction" of unbound radioligand, B_{max} is the density of receptor, K_d is the dissociation constant for the radioligand, and F_i and K_{di} are the free concentration and the dissociation constant of the competing endogenous ligand, respectively. We showed BP values of each VOI in Table 1. Group differences in BP values of the extrastriatal regions between patients and controls were compared using a two-tailed t test.

Table 1
Binding potential (BP) values for regions of interest[a]

Region		BP values	
		Controls (n=19)	Patients (n=10)
Prefrontal cortex	Right	1.07 ± 0.29	0.99 ± 0.15
	Left	1.04 ± 0.29	0.98 ± 0.16
	Right+left	1.05 ± 0.29	0.98 ± 0.15
Temporal cortex	Right	1.74 ± 0.30	1.70 ± 0.23
	Left	1.74 ± 0.30	1.83 ± 0.33
	Right+left	1.74 ± 0.30	1.75 ± 0.29
Parietal cortex	Right	1.20 ± 0.35	1.19 ± 0.19
	Left	1.18 ± 0.33	1.17 ± 0.23
	Right+left	1.19 ± 0.34	1.18 ± 0.21
Thalamus	Right	3.55 ± 0.55	3.32 ± 0.38
	Left	3.54 ± 0.51	3.30 ± 0.44
	Right+left	3.54 ± 0.45	3.30 ± 0.26
Hippocampus	Right	1.53 ± 0.44	1.46 ± 0.43
	Left	1.60 ± 0.41	1.52 ± 0.40
	Right+left	1.67 ± 0.34	1.49 ± 0.30
Anterior cingulate	–	1.17 ± 0.12	0.97 ± 0.17
Midbrain/ventral tegmentum	–	2.26 ± 0.44	2.37 ± 0.31

[a] Values are mean ± SD.

2.4. Network model analysis with structural equation modeling

The present study used structural equation modeling to evaluate the connectivity of regional D2 receptor binding in patients with schizophrenia and normal controls (McIntosh and Gonzalez-Lima, 1994; McIntosh et al., 1994; Horwitz et al., 1999). This computational method allows for the assessment of changes in the inter-regional associations of entire systems. When applied to neural systems, structural equation modeling combines information about anatomical pathways and the correlation coefficients of regional data between brain regions so as to identify the regional associations in a given condition. The correlations between areas are decomposed for assigning numerical weights (path coefficients) to anatomical connections, a process that produces a network model. The technical definition of a path coefficient (expressed in terms of neural pathways) is the direct proportional influence that one region has on another region through their direct anatomical connection, with all other regions in the model left unchanged. A path coefficient is the expected change in the activity of one region given a unit change in the region

influencing it (McIntosh and Gonzalez-Lima, 1994). In this study, the path coefficient indicates the relation of D2 receptors of one region to another through synaptic connections. Brain areas may associate with one another and compose a network with many regions, and large inter-regional covariances of any two regions can come about by not only direct but also indirect relations. Structural equation modeling describes the nature of inter-regional connections by expressing them as directional influences based on the hypothesis-generating model, and it can solve this interpretational problem for the correlations paradigm.

The inter-regional correlations of BP values and the anatomical model were combined using AMOS (version 4, SPSS, Inc.) to create structural equation models (Arbuckle and Wothke, 1995) that determined the path coefficients for each connection. We set the value of proportion of total variance in each region not accounted for by the effect of other regions. We fixed the values at 0.35–0.5 for a given brain region, and modified them if this improved the fit of the model (McIntosh and Gonzalez-Lima, 1994).

In the construction of the network model, we hypothesized that the dopaminergic system in the prefrontal cortex affected that of the anterior cingulate directly or indirectly via other cortical and limbic regions such as the thalamus or hippocampus, since the prefrontal cortex was thought to play some role in subcortical dopamine release in previous studies (Karreman and Moghaddam, 1996), and the anterior cingulate has direct neural input from the prefrontal cortex, temporo–parietal cortex (Vogt and Pandya, 1987), hippocampus (Tamminga et al., 2000) and thalamus (Vogt et al., 1987). Further, we also considered the connections from the midbrain/ventral tegmental area to other regions, since this area affects the limbic and cortical dopaminergic systems as the source of dopaminergic projections (Oades and Halliday, 1987).

In the first step of the construction, by the above hypothesis and the known neuroanatomy (Goldman-Rakic, 1987; Vollenweider, 1998; Steriade, 2001), we developed an initial network model in which it was decided that the path coefficient for feed-forward connectivity was from the prefrontal cortex to the anterior cingulate cortex directly, or indirectly via other cortical and limbic regions. Between the temporal and parietal cortex and the hippocampus and the thalamus, we applied reciprocal connections (Fig. 3a). In the next step, we included the path coefficients from the midbrain/ventral tegmental area to other regions (Fig. 3b), and in the last step, the influence of alternative path connections was estimated and included if it significantly improved the fit of the model with the chi-square statistics (Fig. 3c).

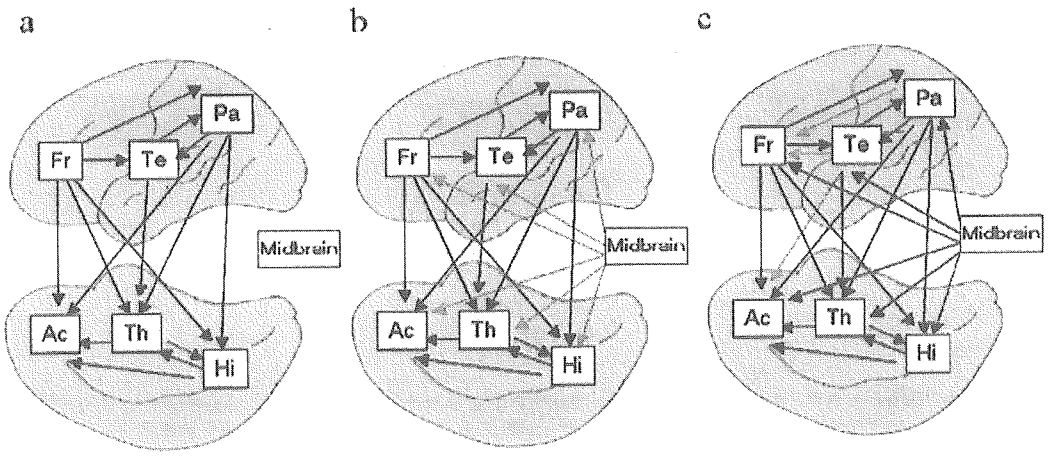

Fig. 3. (a) An initial network model developed under consideration of the known neuroanatomy, where it was decided to illustrate the path coefficients for feed-forward connections from the prefrontal cortex to the anterior cingulate via other cortical and limbic regions. (b) Modified model that included the connections from the midbrain/ventral tegmental area to other regions. (c) Test model in which the influence of alternative path connections was estimated and included if it significantly improved the fit of the model with the chi-square statistics. Red arrows indicated the added path connections to the initial and modified network models.

The networks for the patients and controls were compared using the stacked model approach under the null hypothesis that a single estimate for each path coefficient is adequate for both groups, where instead of estimating a model for each group separately, the models are combined in a single program run (McIntosh and Gonzalez-Lima, 1994; Arbuckle and Wothke, 1995). The process involves statistically comparing functional models using the chi-square goodness-of-fit index of model fit, whereby path coefficients are constrained to be equal between conditions (null model) with those in which the coefficients are allowed to differ (alternative model). The comparison of models is made by subtracting the chi-square value for the alternative model from the chi-square value for the null model. If the alternative model, in which the coefficients were allowed to differ between groups, had a significantly lower chi-square value, then the coefficients that were allowed to vary between conditions were statistically different (McIntosh and Gonzalez-Lima, 1994). A P value of 0.05 (two-tailed) was chosen as the significant threshold.

3. Results

The t-test revealed that the BP value in the anterior cingulate was significantly different in patients with schizophrenia compared with normal controls (mean ± SD: controls, 1.17 ± 0.12, patients, 0.97 ± 0.17, $t_{27}=3.77$, $P=0.001$). There were no significant group differences in any other regions ($P>0.05$). In the analysis of structural equation modeling, our hypothesized model was valid and fit the data well under the null hypothesis that the model fit the data [$\chi^2(10)=16.4$, $P>0.09$, Akaike Information Criteria (AIC)=136.4]. The influence of

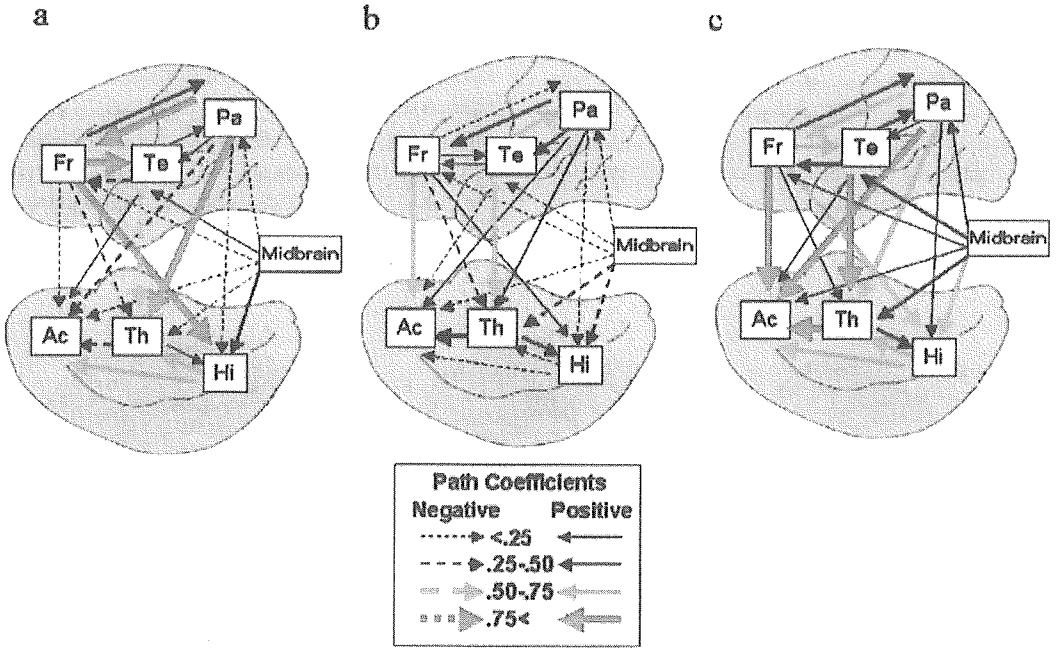

Fig. 4. Lateral and medial views of the human brains showing the functional networks reflecting on dopamine D2 receptor binding for each group, and the differences between groups. Arrows represent path coefficients. The arrow width for each path indicates the strength of each connection. Values for the width gradient are given in the box at the bottom. Positive path coefficients are shown as solid arrows, and negative path coefficients as dashed arrows. Differences are represented as the absolute values calculated by subtracting the coefficients for controls from those of patients. The width of the arrow indicates the magnitude of the difference. The color red indicates relatively large coefficients or differences (>0.75), and moderate coefficients or differences are indicated by the color orange (0.50–0.75). Path coefficients and their differences between groups are also shown in Table 3. Fr: Prefrontal cortex, Te: Temporal cortex, Pa: Parietal cortex, Hi: Hippocampus, Th: Thalamus, Ac: Anterior cingulate, Midbrain: Midbrain/Ventral tegmental area.

Table 2
Correlation matrices of regional BP in healthy control subjects and schizophrenic patients

	Fro	Tem	Par	Hip	Thal	Midbrain	Acing
Controls							
Fro	1.00						
Tem	0.87	1.00					
Par	0.84	0.83	1.00				
Hip	0.55	0.47	0.45	1.00			
Thal	0.15	0.07	0.29	0.46	1.00		
Midbrain	−0.26	−0.05	−0.17	0.25	0.10	1.00	
Acing	−0.37	−0.35	−0.55	−0.02	−0.37	0.11	1.00
Schizophrenics							
Fro	1.00						
Tem	0.52	1.00					
Par	0.53	0.73	1.00				
Hip	0.28	0.45	0.28	1.00			
Thal	0.06	0.53	0.45	0.33	1.00		
Midbrain	−0.18	0.61	−0.16	−0.47	−0.40	1.00	
Acing	0.71	0.64	0.71	0.17	0.57	−0.33	1.00

These values were the input for the path analysis, the results of which are shown in Table 3 and Fig. 4[a].

[a] Fro: Prefrontal cortex, Tem: Temporal cortex, Par: Parietal cortex, Hip: Hippocampus, Thal: Thalamus, Midbrain: Midbrain/Ventral tegmental area, Acing: Anterior cingulate.

alternative path connections did not improve the fit of the model.

Table 3 and Fig. 4 show the connectivity of the regional D2 receptor binding for each group (the correlations used are given in Table 2). The network model of the patients and normal subjects proved to be significantly different between the groups [$\chi^2_{diff}(23)=47.6$, $P<0.005$].

Normal subjects showed relatively large positive path coefficients (>0.75) from parietal cortex to frontal cortex and frontal cortex to temporal cortex among cortical regions, and frontal cortex to hippocampus and hippocampus to anterior cingulate. There were moderate positive coefficients (0.50–0.75) from hippocampus to thalamus and anterior cingulate, and negative coefficients from temporal cortex to thalamus (Table 3, Fig. 4, controls).

On the other hand, patients with schizophrenia showed different path coefficients from controls among regions. There were moderate positive path coefficients from temporal to parietal cortex, temporal

Table 3
Effects decomposition of inter-regional connections in the structural equation model of normal controls and patients[a]

Regions	Prefrontal cortex	Temporal cortex	Parietal cortex	Hippocampus	Thalamus	Anterior cingulate
Prefrontal cortex	–	0.82	0.26	0.75	−0.35	−0.24
	–	0.11	−0.02	0.24	−0.35	0.53
	–	0.71	0.28	0.51	0	0.77
Temporal cortex	−0.28	–	0.11	–	−0.60	0.11
	0.18	–	0.53	–	0.58	−0.07
	0.46	–	0.42	–	1.18	0.18
Parietal cortex	0.91	0.09	–	−0.14	0.80	−0.49
	0.41	0.29	–	−0.04	0.25	0.26
	0.50	0.20	–	0.10	0.55	0.75
Hippocampus	–	–	–	–	0.58	0.50
	–	–	–	–	−0.13	−0.12
	–	–	–	–	0.71	0.62
Thalamus	–	–	–	0.02	–	−0.35
	–	–	–	0.34	–	0.42
	–	–	–	0.32	–	0.77
Midbrain	−0.09	0.14	−0.07	0.31	−0.02	−0.10
	−0.07	−0.12	−0.03	−0.27	−0.35	−0.03
	0.02	0.26	0.04	0.58	0.33	0.07

Horizontal rows list structures being affected, and vertical columns list the origin of the effect. The effects not estimated are indicated by a dash (–). Bold characters represent moderate to large differences of coefficients (>0.50) between normal controls and patients with schizophrenia. Graphic representation of the network structure is shown in Fig. 4.

[a] Within each horizontal row, the upper value is the coefficient of normal controls, the middle value is that of patients, and the lower value is the absolute value calculated by the subtraction of the coefficients of controls from those of patients.

cortex to thalamus, and frontal cortex to anterior cingulate (Table 3, Fig. 4, patients).

The difference of path coefficients was presented as the absolute value calculated by subtraction of the coefficients for controls from those of patients (Table 3). Fig. 4 shows that there was a relatively large difference of path coefficients (>0.75) from frontal cortex, parietal cortex and thalamus to anterior cingulate, and from temporal cortex to thalamus. In addition, there were moderate differences of path coefficients (0.50–0.75) from prefrontal cortex and midbrain to hippocampus, hippocampus to thalamus and anterior cingulate, frontal cortex to temporal cortex, and parietal cortex to frontal cortex and thalamus (Table 3, Fig. 4, differences).

4. Discussion

This is the first study to apply structural equation modeling to data on regional receptor binding, which could be assumed to influence each other and change over the long duration of the disease via the structural network. The results indicated that the network model of the patients and normal subjects differed significantly between the groups.

As to the individual path coefficients, (a) effective connectivity between cortical regions was different between controls and patients; (b) connectivity from prefrontal cortex, parietal cortex, and thalamus to anterior cingulate in patients differed from that in controls; (c) there was no effective connectivity from prefrontal cortex to anterior cingulate and thalamus via the hippocampus in patients as observed in normal subjects; (d) a difference was also observed in the connectivity the temporal cortex and parietal cortex to thalamus, and from the midbrain/tegmental area to hippocampus. These results showed that patients exhibited an abnormality that was not evident in regional receptor binding but was evident through inter-regional connectivity of receptor systems.

This difference is not likely to be due to an effect of blood flow, since BP values from the reference tissue model are minimally dependent on tracer delivery (Lammertsma and Hume, 1996). We think that the scan represents not phasic but tonic dopamine and that there was almost no effect of stressors or internal/external stimuli during the PET scan, since our previous study revealed that extrastriatal [^{11}C]FLB457 was not sensitive to endogenous dopamine (Okauchi et al., 2001). In the previous study, we also found very good test–retest reproducibility for [^{11}C]FLB457 binding in repeated measurements under the same conditions as in this study (Sudo et al., 2001).

Although connecting tracts, including cortico–cortical and thalamo–cortical association fibers, utilize glutamate as a transmitter (Huntley et al., 1994), the dopaminergic and glutamatergic systems are closely integrated, as each modulates the activity levels of the other (Biggs and Starr, 1997). Dopaminergic neurons have input to inhibitory GABAergic neurons of the cortex, and "mis-wiring" of this input was indicated in patients with schizophrenia (Benes, 1997). Taking these findings into consideration, the connections between regional D2 receptor systems might reflect connections between dopamine and several other neurotransmitter systems and affect the dopaminergic tone among several brain regions. Their anomalies may reflect aberrant changes in the structural neuronal network regulating neurotransmitter systems and affect the connectivity of regional D2 receptor systems in patients with schizophrenia.

The absolute values of the path coefficients may indicate the strength of the influence between regions. As to the positive and negative signs of path coefficients, they showed the opposite influence of dopamine neurons from one region to another through the synaptic connections between dopamine and glutamatergic/GABAergic systems. This was supported by the suggestion that dopamine neurons were affected by glutamatergic neurons either directly or via GABAergic interneurons, acting as accelerators and brakes, respectively (Carlsson et al., 2000). However, an increase of post synaptic BP can result from an up-regulation to the decrease in the amount of dopamine or an adaptation to the increase in the amount of dopamine in the synaptic cleft. This does not allow a direct translation of path coefficients based on BP data as indices of excitation or inhibition of the dopaminergic systems. Path coefficients can indicate whether there are group-related differences in functional influences within the same anatomical pathways, but we must evaluate their neurophysiological meaning cautiously under the consideration of interpretative difficulties.

In schizophrenia, aberrant functional integration may appear through the systems-level neuronal changes reflected in the connectivity of regional D2 receptor binding. Aberrant connectivity from the prefrontal cortex, parietal cortex, and thalamus to the anterior cingulate was observed in schizophrenia patients. We considered that the regions without evident change in D2 receptors were also related to the pathophysiology of schizophrenia through aberrant neuronal connections by their effect on dopaminergic regulation in the anterior cingulate, where the change in dopamine D2 receptor binding was shown to be related to the positive symptoms of schizophrenia (Suhara et al., 2002).

Further, it was suggested that defective interactions of the cortico–cortical and cortico–thalamic network might underlie certain dysfunctions of conscious integration such as those seen in schizophrenia (Tononi and Edelman, 2000). The effective connectivity from the prefrontal cortex to limbic regions via the hippocampus observed in normal subjects may relate to normal information processing and cognitive memory function, and aberrant circuitry via the hippocampus may induce deficits in them (Benes, 2000; Fletcher, 1998).

The results suggest that a systems-level change reflected in the connectivity of regional D2 receptor binding was observed in patients with schizophrenia. This change may reflect imbalance and abnormal synaptic connections. However, a few confounding factors need to be considered when interpreting our results. Since the method is a modeling technique, it requires simplifying assumptions about the direction of influences and anatomy. Thus our results were affected by these constraints placed upon our assumptions, although the model fit the data well and the influence of alternative path connections did not improve the fit of the model.

The mean voxel values of the right and left VOIs were used to increase the signal-to-noise ratio for the calculations and to simplify the assumptions and the model regarding the direction of influences and anatomy. As shown in Table 1, the standard deviation in the thalamus and hippocampus was smaller when the values of right and left VOIs were averaged. In all regions, we found a relatively high correlation of the BP values of the right and left VOIs in each group ($r>0.90$), and there may be no serious problem concerning the averaging of the right and left VOIs in these regions. However, we found a trend of asymmetry of the BP values in the temporal regions of the patient group (paired t-test, $t=3.67$, $P<0.01$), and there was the possibility that averaging the right and left VOIs masked asymmetries in the patient group, limiting the conclusions drawn from the model.

Because of the limited number of patients and the moderate level of severity, it cannot be ruled out that, with a larger patient population, other connectivities might also show differences. Although FLB 457 has affinity for both dopamine D2 and D3 receptors, the anatomical distribution of D3 receptors supports the view that the [^{11}C]FLB 457 binding in our measured regions mainly represents binding to D2 receptors (Landwehrmeyer et al., 1993; Murray et al., 1994). Still, there is the possibility that our findings could be partly explained by a change in dopamine D3 receptors.

Although the striatum was regarded as important for the dopaminergic network, we could not evaluate it because of methodological problems. Although [^{11}C]FLB 457 accumulated to a high degree in the striatum, high-affinity ligands show very slow clearance from the high density receptor region where radioligand delivery can be rate-limiting (Farde et al., 1997; Suhara et al., 1999). The connectivity shown in this study may include the effect of unexamined critical regions behind our network model, and we think that our data are currently limited for drawing general conclusions, and future work with ligands better suited for the measurement of extensive brain regions is necessary to solve this problem.

Acknowledgments

We thank T. Saijo, T. Ando, A. Yamamoto, Y. Asai, S. Ito and T. Nakayama for their help in data acquisition. This study was supported by the PET project of the National Institute of Radiological Sciences in Chiba, Japan.

References

Arbuckle, J.L., Wothke, W., 1995. Amos 4.0 User's Guide. Small Waters Corporation, Chicago.

Benes, F.M., 1997. The role of stress and dopamine–GABA interactions in the vulnerability for schizophrenia. Journal of Psychiatric Research 31, 257–275.

Benes, F.M., 2000. Emerging principles of altered neural circuitry in schizophrenia. Brain Research: Brain Research Reviews 31, 251–269.

Biggs, C.S., Starr, M.S., 1997. Dopamine and glutamate control each other's release in the basal ganglia: a microdialysis study of the entopeduncular nucleus and substantia nigra. Neuroscience and Biobehavioral Reviews 21, 497–504.

Carlsson, A., Waters, N., Waters, S., Carlsson, M.L., 2000. Network interactions in schizophrenia–therapeutic implications. Brain Research: Brain Research Reviews 31, 342–349.

Della-Maggiore, V., Sekuler, A.B., Grady, C.L., Bennett, P.J., Sekuler, R., McIntosh, A.R., 2000. Corticolimbic interactions associated with performance on a short-term memory task are modified by age. Journal of Neuroscience 20, 8410–8416.

Farde, L., Suhara, T., Nyberg, S., Karlsson, P., Nakashima, Y., Hietala, J., Halldin, C., 1997. A PET-study of [^{11}C]FLB 457 binding to extrastriatal D2-dopamine receptors in healthy subjects and antipsychotic drug-treated patients. Psychopharmacology 133, 396–404.

Fletcher, P., 1998. The missing link: a failure of fronto–hippocampal integration in schizophrenia. Nature Neuroscience 1, 266–267.

Friston, K.J., Holmes, A.P., Worsley, K.J., Poline, J.P., Frith, C.D., Frackowiak, R.S.J., 1995. Statistical parametric maps in functional imaging: a general linear approach. Human Brain Mapping 2, 189–210.

Goldman-Rakic, P.S., 1987. Circuitry of primate prefrontal cortex and regulation of behavior by representational memory. In: Plum, F., Mountcastle, V. (Eds.), Handbook of Physiology: The Nervous System. Williams & Wilkins, Baltimore, pp. 373–417.

Goncalves, M.S., Hall, D.A., Johnsrude, I.S., Haggard, M.P., 2001. Can meaningful effective connectivities be obtained between auditory cortical regions? Neuroimage 14, 1353–1360.

Horwitz, B., McIntosh, A.R., Haxby, J.V., Furey, M., Salerno, J.A., Schapiro, M.B., Rapoport, S.I., Grady, C.L., 1995. Network analysis of PET-mapped visual pathways in Alzheimer type dementia. Neuroreport 6, 2287–2292.

Horwitz, B., Tagamets, M.A., McIntosh, A.R., 1999. Neural modeling, functional brain imaging, and cognition. Trends in Cognitive Sciences 3, 91–98.

Huntley, G.W., Vickers, J.C., Morrison, J.H., 1994. Cellular and synaptic localization of NMDA and non-NMDA receptor subunits in neocortex: organizational features related to cortical circuitry, function and disease. Trends in Neurosciences 17, 536–543.

Jennings, J.M., McIntosh, A.R., Kapur, S., Zipursky, R.B., Houle, S., 1998a. Functional network differences in schizophrenia: a rCBF study of semantic processing. Neuroreport 9, 1697–1700.

Jennings, J.M., McIntosh, A.R., Kapur, S., 1998b. Mapping neural interactivity onto regional activity: an analysis of semantic processing and response mode interactions. Neuroimage 7, 244–254.

Karreman, M., Moghaddam, B., 1996. The prefrontal cortex regulates the basal release of dopamine in the limbic striatum: an effect mediated by ventral tegmental area. Journal of Neurochemistry 66, 589–598.

Lammertsma, A.A., Hume, S., 1996. Simplified reference tissue model for PET receptor studies. Neuroimage 4, 153–158.

Landwehrmeyer, B., Mengod, G., Palacios, J.M., 1993. Dopamine D3 receptor mRNA and binding sites in human brain. Brain Research: Molecular Brain Research 18, 187–192.

Louilot, A., Le Moal, M., Simon, H., 1989. Opposite influences of dopaminergic pathways to the prefrontal cortex or the septum on the dopaminergic transmission in the nucleus accumbens. An in vivo voltammetric study. Neuroscience 29, 45–56.

McIntosh, A.R., Gonzalez-Lima, F., 1994. Structural equation modeling and its application to network analysis in functional brain imaging. Human Brain Mapping 2, 2–22.

McIntosh, A.R., Grady, C.L., Ungerleider, L.G., Haxby, J.V., Rapoport, S.I., Horwitz, B., 1994. Network analysis of cortical visual pathways mapped with PET. Journal of Neuroscience 14, 655–666.

Murray, A.M., Ryoo, H., Gurevich, E., Joyce, J.N., 1994. Localization of dopamine D3 receptors to mesolimbic and D2 receptors to mesostriatal regions of human forebrain. Proceedings of the National Academy of Sciences of the United States of America 91, 11271–11275.

Oades, R.D., Halliday, G.M., 1987. Ventral tegmental (A10) system: neurobiology: 1. Anatomy and connectivity. Brain Research 434, 117–165.

Okauchi, T., Suhara, T., Maeda, J., Kawabe, K., Obayashi, S., Suzuki, K., 2001. Effect of endogenous dopamine on extrastriate [^{11}C]FLB 457 binding measured by PET. Synapse 41, 87–95.

Simon, H., Taghzouti, K., Gozlan, H., Studler, J.M., Louilot, A., Herve, D., Glowinski, J., Tassin, J.P., Le Moal, M., 1988. Lesion of dopaminergic terminals in the amygdala produces enhanced locomotor response to D-amphetamine and opposite changes in dopaminergic activity in prefrontal cortex and nucleus accumbens. Brain Research 447, 335–340.

Steriade, M., 2001. The GABAergic reticular nucleus: a preferential target of corticothalamic projections. Proceedings of the National Academy of Sciences of the United States of America 98, 3625–3627.

Sudo, Y., Suhara, T., Inoue, M., Ito, H., Suzuki, K., Saijo, T., Halldin, C., Farde, L., 2001. Reproducibility of [^{11}C]FLB 457 binding in extrastriatal regions. Nuclear Medicine Communications 22, 1215–1221.

Suhara, T., Sudo, Y., Okauchi, T., Maeda, J., Kawabe, K., Suzuki, K., Okubo, Y., Nakashima, Y., Ito, H., Tanada, S., Halldin, C., Farde, L., 1999. Extrastriatal dopamine D2 receptor density and affinity in the human brain measured by 3D PET. International Journal of Neuropsychopharmacology 2, 73–82.

Suhara, T., Okubo, Y., Yasuno, F., Sudo, Y., Inoue, M., Ichimiya, T., Nakashima, Y., Nakayama, K., Tanada, S., Suzuki, K., Halldin, C., Farde, L., 2002. Decreased dopamine D2 receptor binding in the anterior cingulate cortex in schizophrenia. Archives of General Psychiatry 59, 25–30.

Sulzer, D., Joyce, M.P., Lin, L., Geldwert, D., Haber, S.N., Hattori, T., Rayport, S., 1998. Dopamine neurons make glutamatergic synapses in vitro. Journal of Neuroscience 18, 4588–4602.

Tamminga, C.A., Vogel, M., Gao, X.-M., Lahti, A.C., Holcomb, H., 2000. The limbic cortex in schizophrenia: focus on the anterior cingulate. Brain Research: Brain Research Reviews 31, 364–370.

Tononi, G., Edelman, G.M., 2000. Schizophrenia and the mechanisms of conscious integration. Brain Research: Brain Research Reviews 31, 391–400.

Vogt, B.A., Pandya, D.N., 1987. Cingulate cortex of rhesus monkey: II. Cortical afferents. Journal of Comparative Neurology 262, 271–289.

Vogt, B.A., Pandya, D.N., Rosene, D.L., 1987. Cingulate cortex of the rhesus monkey: I. Cytoarchitecture and thalamic afferents. Journal of Comparative Neurology 262, 256–270.

Vollenweider, F.X., 1998. Advances and pathophysiological models of hallucinogenic drug actions in humans: a preamble to schizophrenia research. Pharmacopsychiatry 31, 92–103.

Yasuno, F., Hasnine, A.K., Suhara, T., Ichimiya, T., Sudo, Y., Inoue, M., Takano, A., Ou, T., Ando, T., Toyama, H., 2002. Template-based method for multiple volumes of interest of human brain PET images. Neuroimage 16, 577–586.

精神神経学雑誌　第107巻第3号（2005）　235-247頁

原　著

統合失調症患者の視覚情報における前注意的処理の障害について

小嶋　和重，片山　征爾，高木　美和，
吉岡　伸一，川原　隆造

A Deficit in Preattentive Processing of Visual Information in Schizophrenic Patients

Kazushige Kojima, Seiji Katayama, Miwa Takaki,
Shin-ichi Yoshioka, Ryuzou Kawahara :

統合失調症と情報処理の障害との関連が指摘されている．統合失調症患者は視覚的な注意機能が障害されているとの報告がいくつかみられる．注意機能は前注意的処理と注意的処理の2段階から成るといわれている．前注意的処理によって一つずつの走査をしなくても標的を弁別することができる．妨害刺激が増えても探索時間はほぼ一定である．一方，注意的処理は刺激を次々に走査する必要がある．そのため妨害刺激が増えるほど探索時間は長くなる．

本研究では，統合失調症患者30名と健常者30名を対象に視覚弁別課題を用いて前注意的処理機能を検証した．被検者には2種類の視覚探索課題を課し，標的を見つけたらボタンを押すよう教示した．課題図版は5，17，35個の‘X’の中にひとつだけ‘L’が入ったpop-out強図版と5，17，35個の‘T’の中にひとつだけ‘L’が入ったpop-out弱図版で構成された．Pop-out強図版における課題成績は前注意的機能を反映する．アイマークレコーダーを用いて，ボタンを押すまでに要した時間（ボタン押し時間），視点が標的に到達するまでの時間（視点到達時間），最初の眼球運動の方向を記録した．

統合失調症群のボタン押し時間と視点到達時間は，pop-outの強さに関係なく健常群より遅れたが，前注意処理の障害を示す結果は得られなかった．しかし，pop-out強図版において，最初の眼球運動が標的へ向かう割合（的中率）が，統合失調症群は健常群よりも有意に低かった．

これらの結果より，統合失調症患者は前注意的処理に障害があり，初期の眼球運動が誤った方向に誘導されると推察された．

＜索引用語：統合失調症，前注意的処理，pop-out，眼球運動＞

I．はじめに

統合失調症の認知・情報処理の障害については，古くからさまざまな特徴が指摘されている．Kraepelin[18]は著書の中で統合失調症の思考障害について触れており，Bleuler[4]は連合弛緩を統合失調症に特異的な症状と位置づけた．またShakow[29]は，統合失調症患者は外界の刺激に対する積極的な構え（major Set）に問題があると指摘した．

近年の認知心理学的研究においては，人は情報の入力・処理・出力を行う一種の情報処理システムとみなされる．人の情報処理能力には限界があ

著者所属：鳥取大学医学部精神医学教室，Division of Neuropsychiatry, Department of Multidisciplinary Internal Medicine, Faculty of Medicine, Tottori University